Pergamon

Journal of Pharmaceutical & Biomedical Analysis, Vol. 12, No. 1, pp. 65–71, 1994
Elsevier Science Ltd

0731–7085/94 $6.00 + 0.00

Conformational study of cyclo[Gln-Trp-Phe-Gly-Leu-Met] as NK-2 antagonist by NMR and molecular dynamics

TERUNA J. SIAHAAN* and KAREN LUTZ

Department of Pharmaceutical Chemistry, The University of Kansas, Lawrence, KS 66045, USA

Abstract: Cyclo[Gln-Trp-Phe-Gly-Leu-Met] (**1**) is a selective peptide antagonist of NK-2 receptors. The conformational analysis of this peptide was conducted using nuclear magnetic resonance (NMR) and molecular dynamics. This study improves understanding of the neurokinin ligand–receptor interactions. Two-dimensional Homonuclear Hartmann–Hahn (2D-HOHAHA) and rotating frame Overhauser enhancement spectroscopy (2D-ROESY) were used to assign all the protons and to obtain through-space proton–proton interactions. ROE (rotating frame Overhauser enhancement) constraints molecular dynamics were done to find the conformation which is consistent with the NMR data. Two βI (or βV') turns around Trp-2-Phe-3 and around Leu-5-Met-6 are found in this peptide which are represented by models. The conformation of this peptide is also compared with the non-peptide NK-2 antagonist SR-48968 (**2**).

Keywords: *Cyclo[Gln-Trp-Phe-Gly-Leu-Met]; cyclic peptide; conformation; NMR, molecular dynamics; NK-2 antagonist; neurokinins.*

Introduction

Neurokinins (tachykinins) are a family of neuropeptides which have been investigated since the discovery of substance P [1]. Since then, two other neurokinins, neurokinin A (NKA) and neurokinin B (NKB) have been discovered [2]. Neurokinins are involved in a variety of biological functions such as smooth muscle constriction, pain and inflammation [1, 2]. Three neurokinin receptors have been isolated for these endogenous ligands: NK-1 receptor for SP, NK-2 receptor for NKA, and NK-3 receptor for NKB; they are members of the G-protein coupled receptor super family [3, 4]. The selectivity of substance P, NKA and NKB toward their respective receptor is presumably due to the amino acid sequence and the peptide conformation. Previous studies showed that the replacement of Phe-7, Phe-8, Leu-10 and Met-11 have the most impact on the biological activity of substance P; this suggests that substance P interacts with its receptor at the C-terminal region [5]. Therefore, the conformational study of this region can improve the understanding of the neurokinins' selectivity.

Many studies have been done to develop peptide, peptidomimetic and non-peptide antagonists for the neurokinins [6–8]; but, the understanding of their selectivity and mechanism of recognition by the receptors has been limited. Cyclo[Gln-Trp-Phe-Gly-Leu-Met] (**1**) [9] and SR48968 (**2**) [7], shown in Fig. 1, are the peptide and non peptide antagonist of NK-2 receptors, respectively, and the conformation of these two compounds will be compared. Cyclo peptide **1** was derived from the C-terminal sequence of substance P where the Trp-2 in this molecule was used to substitute Phe residue in substance P and its selectivity presumably is due to the conformational restriction by N- to C-terminus cyclization. The conformational study of **1** was done by NMR and molecular dynamics simulation and the conformational study of **2** was done by molecular dynamics and energy minimization. This study could possibly help to understand the relationship between the conformation and the biological activity of the peptide and non-peptide neurokinin antagonists.

Materials and Methods

The linear Gln-Trp-Phe-Gly-Leu-Met-OH was synthesized using t-Boc solid-phase peptide synthesis on PAM-resin (Sigma). The C- to N-terminus cyclization was done using the

*Author to whom correspondence should be addressed.

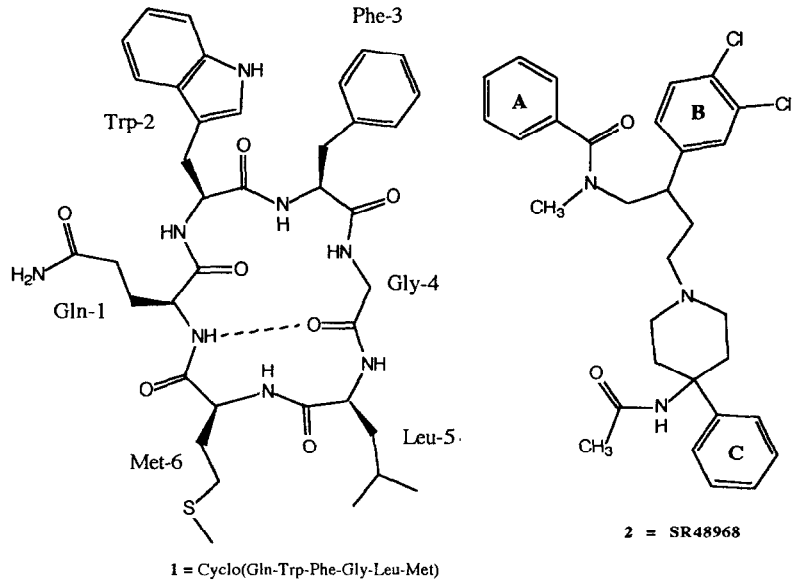

Figure 1
The structure of the peptide antagonist cyclo[Gln-Trp-Phe-Gly-Leu-Met] (**1**) and the non-peptide antagonist SR48968 (**2**).

Table 1
Proton chemical shifts in ppm of cyclo[Gln-Trp-Phe-Gly-Leu-Met] in $DMSO_{d6}$ using DMSO peak as a standard at 2.49 ppm

Residue	NH*	H_α*	H_β*	Others*	NH $\Delta\delta/\Delta T$‡
Gln-1	7.75(d)	3.94(m)	1.82(m)	H_γ: 1.98(m); NH_ϵ: 7.15(s), 6.79(s)	1.56
Trp-2	8.10(d)	4.23(m)	2.98(dd); 3.04(dd)	†Ar = NH: 10.79(s); H_2: 7.04(s); H_4: 7.47(d); H_5: 6.97(t); H_6: 7.07(t); H_7: 7.32(d)	4.18
Phe-3	7.93(d)	4.21(m)	3.05(d)	†Ar = $H_{2,6}$: 7.12(d); $H_{3,5}$: 7.32(t); H_4: 7.15(t)	3.66
Gly-4	8.21(t)	3.61(d)			4.40
Leu-5	8.29(d)	4.13(m)	1.50(m); 1.58(m)	H_γ: 1.54(m); H_δ: 0.82(d), 0.89(d)	4.98
Met-6	8.09(d)	4.14(m)	2.05(m)	H_γ: 2.40(m), 2.47(m); H_ϵ: 2.04(s)	4.22

*The letter in parenthesis is the proton multiplicity (s = singlet; d = doublet; t = triplet; m = multiplets).
†Ar = aromatic rings of Trp-2 and Phe-3.
‡Temperature coefficient of the amide protons in ppb $degree^{-1}$.

procedure explained by Rapoport and co-workers [10]. The cyclic product was purified using silica gel flash column chromatography with 15% PAW (pyridine–acetic acid–water, 55:20:25, v/v/v) in ethyl acetate as a solvent. The pure product of **1** was subjected to Fast Atom Bombardment–Mass Spectroscopy (FAB–MS); this gave a molecular weight of 762 atomic mass units.

All NMR experiments were performed using a Bruker AM-500 (500 MHz) in $DMSO_{d6}$ with peptide concentration of 8.3 mg ml^{-1}. The HOHAHA (Homonuclear Hartmann–Hahn) experiments were done using 70 and 90 ms mixing times [11]. The ROESY (rotating frame Overhauser enhancement spectroscopy) experiments [12] were performed using 100 and 250 ms mixing times at 25°C. Molecular modelling experiments were done using IRIS Silicon Graphics (4D/25G) which were equipped with the Insight/Discover program from Biosym Technologies.

Results and Discussion

The proton assignments were made using 2D-HOHAHA and their chemical shifts are shown in Table 1. The HOHAHA spectrum shows clear connectivity between NH to HC_α, HC_β and HC_γ of Gln-1. The connectivity pattern of NH Met-6 is similar to the NH of Gln-1; but the HC_γ of Met-6 is slightly farther

down field than the HC_γ of Gln-1. The protons of Leu-5 can be distinguished from the protons of other amino acids by their chemical shifts and the connectivity pattern from NH to HC_α, HC_β, HC_γ and HC_δ, and the Gly-4's protons were identified immediately by the triplet shape of the NH proton and its connectivity with the HC_α protons. The connectivity pattern and HC_β's chemical shifts of Trp-2 and Phe-3 are very similar except the NH of Trp-2 is farther downfield than the NH Phe-3. The solvent accessibility of the amide protons was analysed by variable temperature NMR and their temperature coefficients are shown in Table 1. The NH of Gln-1 has a low temperature coefficient, thus the NH can form hydrogen bonding with a CO group in the peptide.

The ROESY spectrum determines the through-space inter-proton distances of cyclo-[Gln-Trp-Phe-Gly-Leu-Met]. Eight inter-residue and 18 intra-residue cross-peaks were found in the ROESY spectrum (Fig. 2). The amide region [Fig. 2(a)] shows medium ROE cross-peaks from the NH of Leu-5 to the NH of Met-6 and from the NH of Met-6 to the NH of Gln-1. The ROEs and temperature coefficient of NH Gln-1 suggest a β-turn at the Leu-5-Met-6 ($i + 1$ and $i + 2$) where the NH of Gln-1 can form a hydrogen bond to the CO of Gly-4 (Fig. 1). A weak ROE cross-peak was observed from the NH of Trp-2 to the NH of Phe-3 which suggests a more flexible β-turn at Trp-2-Phe-3. The backbone flexibility occurs at the Gly-4 residue; this contributes to the lack of ROE between the NH of Phe-3 and the NH of Gly-4. This peptide presumably exists in a conformational equilibrium; this is also reflected in the broad lines of the one dimensional (1D) spectrum. The flexibility of Gly-4 residue is shown by the molecular dynamics simulation (see below).

ROE restrained molecular dynamics simulations [13] were used on cyclo[Gln-Trp-Phe-Gly-Leu-Met] to find a reasonable conformation which is consistent with the ROE data. The inter-proton distances were estimated from the intensity of the cross-peaks from the ROESY experiments. Distance ranges of strong (2–2.5 Å ± 0.5), medium (2.5–3.5 Å ± 0.5) and weak (3.5–4.5 Å ± 0.5) were employed as ROE-constraints in the molecular dynamics simulations for 100 picoseconds (ps) at 900 K; all peptide bonds were kept in the *trans* configuration with torsion force during molecular dynamics. Every 100 femtoseconds (fs) a structure was saved in a history file for analysis after simulation. Conformational changes during the 900 K molecular dynamics were analysed from the history file by plotting phi and psi angles vs time. Twenty structures were selected from this high temperature simulation to represent different conformations. Each conformational representative was subjected to molecular dynamics simulation at 300 K for 20 ps with ROE-constraints, and every 25 fs a structure was saved in a history file. The total energy profile of each molecular dynamics run was plotted against time. Several low energy structures were extracted and minimized with and without ROE-constraints using steepest descent followed by conjugate gradient minimizations until the rms-derivatives equated 0.001 kcal mole-$Å^{-1}$.

The resulting structures from these experiments were analysed and compared to the NMR data. Ten low energy structures from the ROE-constraints molecular dynamics simulation are compared in Fig. 3(a). This peptide can adopt two βI (or βV′) turns at Leu-5-Met-6 and Trp-2-Phe-3 as $i + 1$ and $i + 2$ residues and shows hydrogen bonds from the NH of Gln-1 to the CO of Gly-4. Occasional

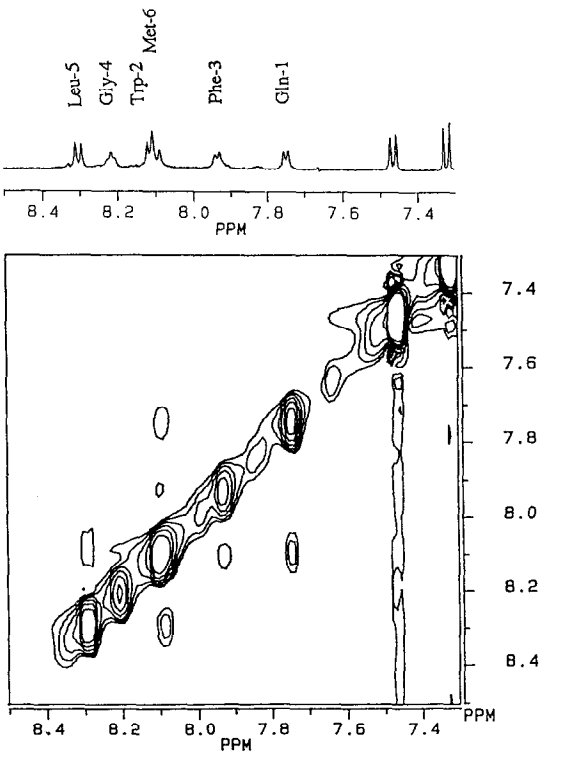

Figure 2(a)

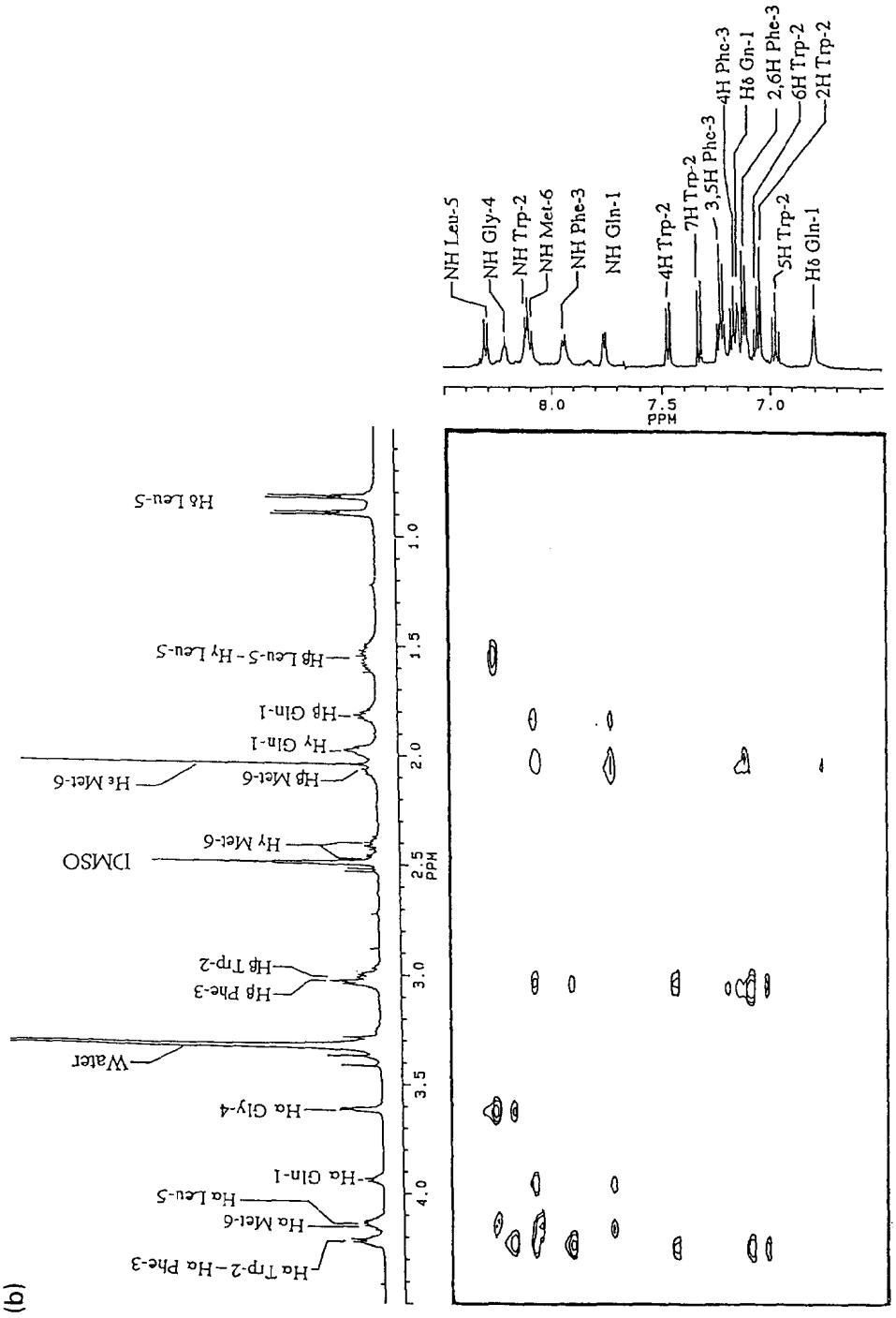

Figure 2
The 2D-ROESY spectra of cyclo[Gln-Trp-Phe-Gly-Leu-Met] (**1**) at 250 ms mixing time. (a) The amide–amide region; (b) the NH to HC_α, HC_β, HC_γ, HC_δ and HC_ϵ.

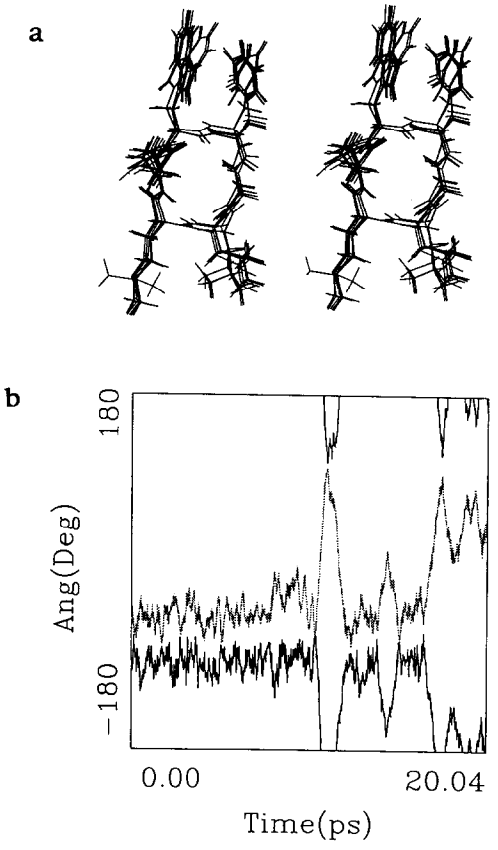

Figure 3
(a) Stereoview of 10 superimposed models for the solution structure of cyclo[Gln-Trp-Phe-Gly-Leu-Met] from 10 different time points in molecular dynamics simulation. (b) The movement of the psi angle of Phe-3 (light line) and the phi angle of Gly-4 (dark line) during 20 ps of ROE-constraints molecular dynamics simulation at 300 K.

hydrogen bonding from the NH of Gly-4 to the CO of Gln-1 was observed during molecular dynamics simulation. The flexibility of the β-turn at Trp-2-Phe-3 was affected by the flexibility of the Gly-4 residue which is shown by the movement of the psi angle of Phe-3 and the phi angle of Gly-4 during molecular dynamics simulation at 300 K [Fig. 3(b)]. One low energy conformer which represents a static structure of this peptide is the model L100 (Fig. 4). The phi and psi angles of this model and the calculated phi angles from $J_{NH-\alpha}$ [14] are shown in Table 2. Furthermore, the comparison between the inter-proton distances of L100 and the observed ROEs are shown in Table 3 and they reflect the degree of consistency between the models and the NMR data. Sumner and coworkers also found a β-turn at Leu-Met in the C-terminal tetrapeptide segment of substance P and physalaemin [15], and they also suggest that the β-turn conformation at the C-terminus is important for biological activity and selectivity.

The conformational recognition of **1** by NK-2 receptors could possibly be due to the recognition of the relative orientation of the

Table 2
Phi and psi angles of cyclo[Gln-Trp-Phe-Gly-Leu-Met] from L100

Structure	L100*	$J_{NH-\alpha}$ (Hz)	Calculated phi†
Phi Gln-1	−87.1	6.3	30, 90, −76, −164
Psi Gln-1	78.0		
Phi Trp-2	62.7	6.3	30, 90, −76, −164
Psi Trp-2	−82.5		
Phi Phe-3	−84.4	7.1	37, 83, −80, −160
Psi Phe-3	−41.9		
Phi Gly-4	−87.4	5.4 + 5.5	38, 132, −38, −132
Psi Gly-4	68.7		
Phi Leu-5	64.7	7.9	45, 74, −85, −155
Psi Leu-5	−74.6		
Phi Met-6	−85.5	7.9	45, 74, −85, −155
Psi Met-6	−50.4		

*Angles in degrees.
†Calculated from $J_{NH-\alpha}$ using ref. 14.

Table 3
The comparison between the observed ROEs and inter-proton distances (Å) from the proposed model (L100)

NH	NH	Int.	L100
Trp-2	Phe-3	w	4.11
Leu-5	Met-6	m	3.94
Met-6	Gln-1	m	2.46
NH	HC_α		
Gln-1	Met-6	m	3.60
Gln-1	Gln-1	w	3.06
Trp-2	Gln-1	s	2.34
Trp-2	Trp-2	s	2.33
Phe-3	Phe-3	s	3.05
Gly-4	Phe-3	m	3.56
Gly-4	Gly-4	w/w	2.52/3.08
Leu-5	Gly-4	s/s	2.54/3.53
Leu-5	Leu-5	w	2.32
Met-6	Met-6	s	3.07
NH	HC_β		
Gln-1	Gln-1	m/m	2.57/2.80
Trp-2	Trp-2	w/w	3.16/3.68
Leu-5	Leu-5	s/s	3.20/3.72
Met-6	Met-6	w/w	2.62/2.84
HC_α	HC_β		
Gln-1	Gln-1	m/m	2.52/3.07
HC_α	HC_γ		
Gln-1	Gln-1	w/w	3.30/3.84

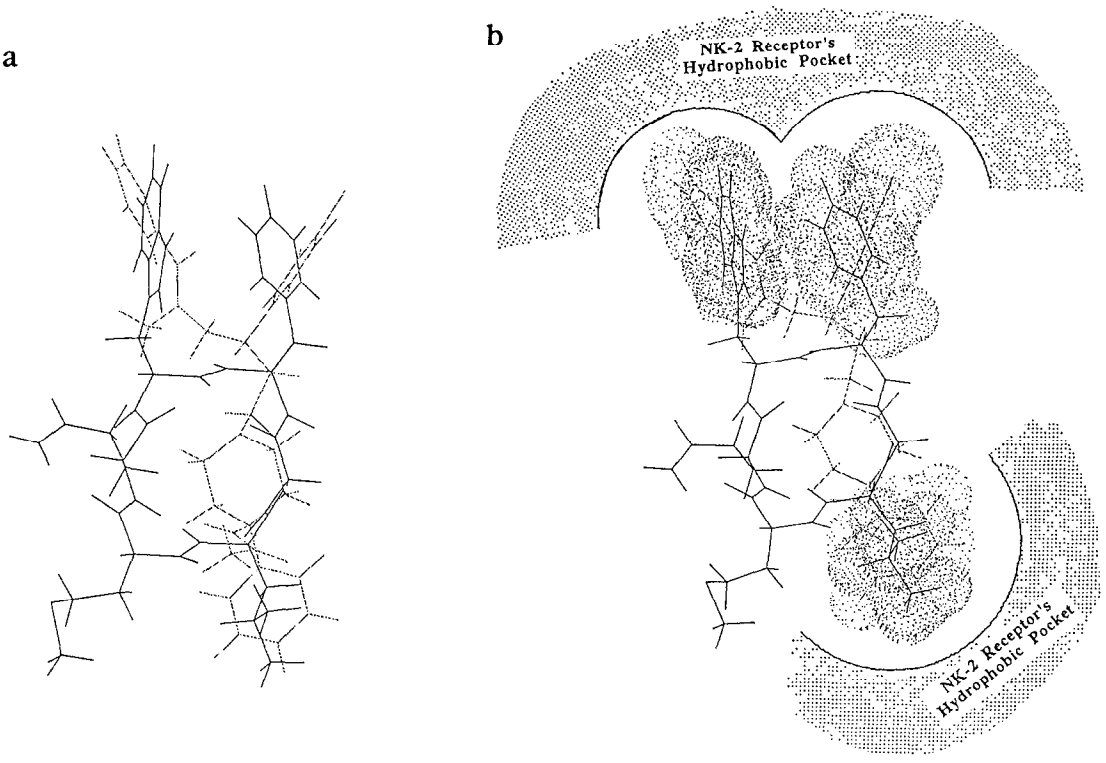

Figure 4
(a) The comparison between the conformation of the peptide **1** (L100, solid line) and the non-peptide **2** (dotted line). (b) The proposed recognition of the peptide (**1**) and the nonpeptide (**2**) antagonists by the hydrophobic pockets of NK-2 receptors.

aromatic rings of Trp-2 and Phe-3 side chains. Both of the side chains of Trp-2 and Phe-3 are in the axial position about the backbone ring in L100 where the aromatic–aromatic interactions occurs between the indole ring of Trp-2 and phenyl ring of the Phe-3. The conformation of **1** was also compared with the low energy conformer of non-peptide antagonist **2** which is shown in Fig. 4(a). Two of the aromatic rings (ring A and ring B, see Fig. 1) in **2** can occupy the same hydrophobic pocket as the indole and phenyl ring in Trp-2 and Phe-3 of **1** as shown in Fig. 4(b). This could suggest that the two close aromatic rings in both **1** and **2** are important for NK-2 recognition. Also, the other aromatic ring C (see Fig. 1) is superimposable with the Leu-5 side chain in peptide **1**, suggesting another hydrophobic pocket in the NK-2 receptor that recognized these two compounds. In conclusion, there is a possibility that the peptide (**1**) and nonpeptide (**2**) antagonists of NK-2 are recognized by the same hydrophobic pockets in the NK-2 receptor. This work could help elucidate and design the selective antagonists to different neurokinin receptors mentioned above.

Acknowledgements — This research was supported by the New Faculty Start-Up Fund to TJS from the Pharmaceutical Chemistry Department and General Research Fund (GRF-3424), The University of Kansas. This research was also supported by American Heart Association, Kansas Affiliate (KS-92-GB-9) and NSF EPSCOR (EHR 92-55223). We thank Dr D. Vander Velde and Dr T. Williams for technical support in the NMR and mass spectroscopies, respectively.

References

[1] B. Pernow, *Pharmacol. Rev.* **35**, 85–141 (1983).
[2] J.E. Maggio, *Ann. Rev. Neurosci.* **11**, 13–28 (1988).
[3] S. Guard and S.P. Watson, *Neurochem. Int.* **18**, 149–165 (1991).
[4] S. Nakanishi, *Ann. Rev. Neurosci.* **14**, 123–136 (1991).
[5] R. Couture, A. Fournier, J. Magnan, S. St.-Pierre and D. Regoli, *Can. J. Physiol. Pharmacol.* **57**, 1427–1435 (1979).
[6] P. Ward, G.B. Ewan, C.C. Jordan, S.J. Ireland, R.M. Hagan and J.R. Brown, *J. Med. Chem.* **33**, 1848–1851 (1990).
[7] S.L. Harbeson, S.A. Shatzer, T.-B. Le and S.H. Buck, *J. Med. Chem.* **35**, 3949–3955 (1992).
[8] K.J. Watling, *TiPS* **13**, 266–269 (1992).
[9] A.T. McKnight, J.J. Maguire, M.A. Varney, B.J. Williams and L.L. Iversen, *Regul. Pept.* **22**, 127 (1988).
[10] J.C. Lagarias, R.A. Houghten and H. Rapoport, *J. Am. Chem. Soc.* **100**, 8202–8209 (1987).

[11] A. Bax and D.G. Davis, *J. Magn. Reson.* **65**, 355–360 (1985).
[12] A. Bax and D.G. Davis, *J. Magn. Reson.* **63**, 207–213 (1985).
[13] R.M. Schek, W.F. van Gunsteren and R. Kaptein, *Methods in Enzymology*, Vol. 117, pp. 204–217. Academic Press, San Diego (1989).
[14] V.F. Bystrov, *Progr. NMR Spectrosc.* **10**, 41–81 (1976).
[15] S.C.J. Sumner, K.S. Gallagher, D.G. Davis, D.G. Covell, R.L. Jernigan and J.A. Ferretti, *J. Biomol. Struct. Dyn.* **8**, 687–707 (1990).

[*Received for review 1 April 1993; revised manuscript received 6 May 1993*]